scientific reports

Check for updates

OPEN

The LncRNA lnc-POTEM-4:14 promotes HCC progression by interacting with FOXK1

Bo Peng[1,2,3,6], Zhipeng Quan[1,2,3,6], Lixing Liang[3,4], Mingjiang Liu[1,2,3], Kai Hu[3,4], Shilian Chen[1,2,3], Qiuli Xie[1,2,3], Jing Qin[3,4], Jingzhao Chen[5], Lijuan Liao[1,2,3], Songqing He[1,2,3]✉ & Zeyuan Li[1,2,3]✉

Hepatocellular carcinoma (HCC) is one of the most common malignant tumours of the digestive tract and poses a serious threat to human life. This study first analysed two GEO datasets (GSE166705 and GSE115018) to screen for differentially expressed lncRNAs between HCC and adjacent tissues. The lncRNA lnc-POTEM-4:14 was determined via a series of methods to be closely related to liver cancer. Further research was subsequently performed to investigate the role of the lncRNA lnc-POTEM-4:14 in the progression of HCC. The lncRNA lnc-POTEM-4:14 is localized primarily within the nucleus and is highly expressed in liver cancer tissues. We established lnc-POTEM-4:14 knockdown and overexpression cell lines to analyse the role of lnc-POTEM-4:14 in liver cancer through functional experiments such as qPCR and WB. We identified FOXK1 as an RNA-binding protein (RBP) of lnc-POTEM-4:14 that participates in MAPK signal activation and cell cycle progression by regulating the activation or expression levels of the downstream target protein TAB1 as a transcription factor. The restoration of FOXK1 can rescue the limited proliferation and increased apoptosis caused by lnc-POTEM-4:14 knockdown. Finally, we validated our hypothesis in a nude mouse tumour-bearing model. In conclusion, lnc-POTEM-4:14 affects the progression of HCC through the FOXK1/TAB1/NLK axis, suggesting that lnc-POTEM-4:14 has potential as a therapeutic target for treating this aggressive malignancy.

Keywords Hepatocellular carcinoma, lnc-POTEM-4:14, FOXK1, TAB1, NLK

Hepatocellular carcinoma (HCC), which accounts for 90% of primary liver cancers, is a diverse and complex disease influenced by multiple aetiological factors. Over 80% of HCC cases are reported in low- to middle-resource regions, particularly Eastern Asia and sub-Saharan Africa, where access to medical resources is often limited[1]. The aetiology of liver cancer encompasses cirrhosis, hepatitis B or C virus infection, excessive alcohol consumption, and nonalcoholic steatohepatitis[2,3]. These factors initiate liver damage, leading to a vicious cycle of destruction and regeneration that fuels inflammation, fibrosis, and ultimately carcinogenesis[4]. An enhanced understanding of the pathogenesis of liver cancer holds promise for the identification of novel diagnostic markers and therapeutic targets, which could ultimately improve clinical treatment efficacy and prognosis.

Long noncoding RNAs (lncRNAs) are a group of transcripts with a length of > 200 nucleotides but lacking canonical coding sequences[5]. LncRNAs have attracted much attention in the last decade because they play important roles in various physiological and pathological processes via interactions with other molecules, such as DNA, RNA and proteins[6,7]. Emerging evidence has suggested the crucial role of lncRNAs in the tumorigenesis and progression of liver cancers. The abnormal expression of several lncRNAs is involved in promoting and maintaining tumour initiation and progression in HCC[8,9]. LncRNAs have potential clinical applications as tumour markers for the diagnosis, treatment, prognosis, and recurrence of HCC. Further investigation will

[1]Division of Hepatobiliary Surgery, the First Affiliated Hospital of Guangxi Medical University, NO 6 Shuangyong Road, Nanning 530021, Guangxi, China. [2]Key Laboratory of Early Prevention and Treatment for Regional High Frequency Tumor (Guangxi Medical University), Ministry of Education, Nanning 530021, Guangxi, China. [3]Guangxi Key Laboratory of Immunology and Metabolism for Liver Diseases, Nanning 530021, Guangxi, China. [4]Department of Radiation Oncology, the First Affiliated Hospital of Guangxi Medical University, Nanning 530021, Guangxi, China. [5]Division of Pathology, The People's Hospital of Guangxi Zhuang Autonomous Region, Nanning 530021, Guangxi, China. [6]Bo Peng and Zhipeng Quan contributed equally to this work. ✉email: dr_hesongqing@163.com; lizeyuan03@126.com

help to develop a better understanding of the function of lncRNAs in HCC and provide general directions and strategies for further research[10].

Interestingly, the subcellular localization of lncRNAs can be dynamic[11] and is a key determinant of their function[12]. Some kinds of lncRNAs, such as nuclear XIST, exist predominantly in the cell nucleus[13], whereas other lncRNAs, such as TINCR, exist mainly in the cytoplasm[14]. To date, there is no consensus on whether lncRNAs are enriched mainly in the nucleus or cytoplasm, with some studies suggesting that lncRNAs are enriched mainly in the nucleus[12,15] and others indicating that lncRNAs are enriched mainly in the cytoplasm[16]. However, the subcellular localization of lncRNAs definitely plays an important role in determining their function. The CCAT1 lncRNA gene can produce two isoforms: the long isoform (CCAT1-L) is nuclear and the short isoform (CCAT1-S) is cytoplasmic, CCAT1-L regulates long-range chromatin interactions at the MYC locus, however, the function of CCAT1-S is unclear[17]. GUARDIN can maintain genomic integrity in both cytoplasmic and nuclear ways[18]. LncRNA HOTAIR was mainly located in the cytoplasm of HCC cells, HOTAIR regulate RAB35 and SNAP23 to promote exosome secretion[19]. The important functional mode of nuclear lncRNAs is binding to RBPs[20], which in turn regulate the fate of cellular RNAs, such as their production, maturation and degradation[21]. Recent studies have revealed the functions of some nuclear lncRNAs. For example, perturbation of the RBP CCT3 and lncRNA LINC00326 regulatory network led to decreased lipid accumulation and increased lipid degradation, diminishing tumour growth in vivo[22]. However, the functions of many nuclear lncRNAs are still unknown. In this study, we explored the function of the nuclear lncRNA lnc-POTEM-4:14 in liver cancer.

FOXK1, a member of the Forkhead box (FOX) gene family[23], is an evolutionarily conserved transcription factor that is recognized as a key transcriptional regulator involved in many types of cancer, including HCC[24]. It has been reported that FOXK1 is significantly upregulated in human HCC. The downregulation of FOXK1 suppressed the proliferation, migration and invasion of HCC cells[25]. To date, lncRNAs have been found to regulate FOKX1 mainly by sponging miRNAs; for example, the lncRNA SNHG1 sponges miR-376a to regulate FOXK1 to affect tumour growth and metastasis in HCC[26].

In our current study, we observed that lnc-POTEM-4:14 (990 bp) was upregulated in HCC tissues; however, its regulatory role in HCC remains largely unknown. Motivated by these findings, we conducted a more in-depth analysis to elucidate its biological significance in HCC progression. Additionally, we examined the underlying molecular mechanisms with the aim of identifying potentially effective diagnostic and therapeutic targets for HCC.

Materials and methods

Clinical patients and tissue specimens

Fresh tumour tissues and adjacent noncancerous tissues were collected from the First Affiliated Hospital of Guangxi Medical University. All participating patients signed relevant informed consent forms prior to surgery. The clinical samples were obtained from 20 hepatocellular carcinoma patients (from 22 initially recruited, excluding two cases based on prior chemotherapy/radiotherapy treatment or postoperative non-HCC pathological diagnosis) undergoing surgery at The First Affiliated Hospital of Guangxi Medical University between September 2022 and February 2023. The obtained tissues were immediately snap-frozen in liquid nitrogen and subsequently stored at -80 °C. This study was approved by the Institutional Ethics Committee of the First Affiliated Hospital of Guangxi Medical University, and all the research was conducted in accordance with government policies and the Declaration of Helsinki.

Cell culture and transfection

The human HCC cell lines LM3, Huh-7, MHCC97H and SNU-449 were purchased from the American Type Culture Collection (ATCC). The cells were cultured in DMEM or RPMI 1640 (Gibco, USA) supplemented with 10% foetal bovine serum (FBS; Gibco, USA) and 1% penicillin/streptomycin (P1400; Solarbio, China) and incubated with 5% CO_2 at 37 °C. All the cell lines were tested regularly for mycoplasma contamination and were utilized within 20 passages. ASO (RiboBio, China) and plasmids (IGEbio, China) were transfected into cells using Lipofectamine 3000 reagent (L3000001, Invitrogen, USA). The ASO sequences are listed in Supplementary Table 3. The plasmids we used was pCDNA 3.4, and the plasmid constructs were obtained from IGE Biotechnology (Guangzhou, China). According to the manufacturer's instructions. First, inoculate the cells at an appropriate density into the culture dish. When the cells grow to 70 – 80% confluence, perform transfection. Mix the plasmid DNA with the liposome transfection reagent (Lipofectamine 3000 + P3000) in a certain proportion, incubate at room temperature for 15 min, and then add the mixture to the cell culture medium. After 48 h of transfection, observe the expression of green fluorescent protein (GFP) through a fluorescence microscope to evaluate the transfection efficiency.

Subcellular fractionation

The nuclear and cytoplasmic fractions were separated using a Minute™ Cytoplasmic and Nuclear Extraction Kit (SC-003, Invent, USA) according to the manufacturer's instructions.

The isolated RNA was reverse transcribed into cDNA, and the expression levels of LINC01977, GAPDH, and U6 in the cytoplasm and nucleus were measured via qPCR. U6 and GAPDH were used as internal controls for nuclear and cytoplasmic proteins, respectively.

Detection of cell proliferation

For the CCK8 assay, we seeded 1000 cells per well into a 96-well plate and allowed them to adhere stably to the surface. Then, we added CCK8 reagent (Dojindo, Japan) and incubated the plate for 2 h in a cell culture incubator. We then measured the absorbance at 450 nm using a microplate reader (BioTek Instruments, USA).

Cell proliferation was also measured via an EdU Cell Proliferation Kit (C0075S, Beyotime, China) following the manufacturer's protocols. The proliferative cells were stained with EdU reagent and Hoechst 33,342 dye to stain the cell nuclei. The fluorescence was imaged on an Olympus IX71 microscope, and each sample was measured at least three times.

Colony formation assays were conducted as follows: cells were seeded in 6-well plates at a density of 500 cells per well and incubated in a cell culture incubator for approximately 10–14 days. Once distinct colonies were visible under a microscope, the cells were fixed with 4% paraformaldehyde and stained with crystal violet. Photographs were taken, and colonies were counted.

Fluorescence in situ hybridization (FISH)

The cells were seeded onto cell culture slides and allowed to fully adhere. Next, they were fixed, permeabilized, and blocked with a prehybridization solution. The cells were then incubated overnight at 4 °C with a biotinylated probe to enable the binding of the probe to its target. Finally, the cell nuclei were stained with DAPI and imaged under a fluorescence microscope (Olympus).

Cell cycle and apoptosis analysis

The cells were collected approximately 48 h after ASO or plasmid transfection and then harvested and stained according to the manufacturer's instructions. For cell cycle detection, a Cell Cycle Staining Kit (CCS012, Liankebio, China) was used, whereas for apoptosis detection, an Annexin V-APC/7-AAD Apoptosis Kit (AP105, Liankebio, China) was used. After staining, the cells were analysed and counted using flow cytometry.

RNA isolation and quantitative real-time PCR (qRT–PCR)

RNAiso Plus (Takara, Japan) reagent was used to extract total RNA, and cDNA was subsequently obtained via MonScript™ RT Mix (MR05101, Monad, China). Detection was performed using MonAmp™ qPCR Mix (MQ00501S, Monad, China) and a CFX96™ Real-Time System (Bio-Rad, USA). The primers used are listed in Supplementary Table 4.

Western blot (WB) and antibodies

WB was conducted according to conventional methods as previously reported[27]. The following antibodies were used: BAX (1:5,000; 50599-2-Ig, Proteintech), BCL2 (1:2,000; 12789-1-AP, Proteintech), c-Caspase3 (1:800; 341034, Zen-bio), CDK2 (1:800; R22532, Zen-bio), Cyclin D1 (1:5,000; 60186-1-Ig, Proteintech), Cyclin E1 (1:800; 340298, Zen-bio), FOXK1 (1:1000; 12025; Cell Signaling Technology), GAPDH (1:5,000; 10494-1-AP, Proteintech), IgG (30000-0-AP, Proteintech), NLK (1:800; R389377, Zen-bio), TAB1 (1:800; R383163, Zen-bio), p-P38 (1:1000; 4511T; Cell Signaling Technology), p-TAK1 (1:1000; 9339 S; Cell Signaling Technology), HRP-conjugated Affinipure goat anti-mouse IgG(H + L) (1:5,000; SA00001-1, Proteintech), and HRP-conjugated Affinipure goat anti-rabbit IgG(H + L) (1:5,000; SA00001-2, Proteintech).

RNA pulldown assay

The RNA pulldown assay was performed using the PureBinding® RNA-Protein Pull-Down Kit (P0201, Geneseed, China). In accordance with the manufacturer's protocol, cell lysates, magnetic beads, biotinylated lnc-POTEM-4:14 and its antisense strand were incubated at 4 °C on a rotator for 1 h. The proteins were then eluted and analysed via mass spectrometry and WB.

RNA immunoprecipitation (RIP) and chromatin immunoprecipitation (ChIP)

The PureBinding® RNA Immunoprecipitation Kit (P0101, Geneseed, China) was used for RIP assays according to the manufacturer's instructions. The BeyoChIP™ Enzymatic ChIP Assay Kit (P2083S, Beyotime, China) was used for ChIP assays according to the manufacturer's protocol.

RNA sequencing

Samples were collected and preserved in TRIzol (three samples in each group), and cDNA libraries were sequenced on the Illumina sequencing platform by MetWare Biotechnology Co., Ltd. (Wuhan, China). Significantly differentially expressed genes were defined as those with a fold change ≥ 2.0 and $P < 0.05$. Bioinformatics analysis was conducted through heatmaps, KEGG enrichment analysis, and other methods.

Immunohistochemistry (IHC)

Fresh tissue was fixed, dehydrated, and embedded in paraffin before being cut into 5 μm sections and mounted on glass slides. The sections were then dewaxed and hydrated, followed by antigen retrieval using Tris-EDTA (pH 9.0). After inactivation of endogenous peroxidase activity and blocking with serum at room temperature, the sections were incubated with Ki67 antibody (1:2000; Proteintech, USA) overnight at 4 °C. After washing, the sections were incubated with a biotinylated secondary antibody (PV-9001, ZSGB-BIO, China) on a shaker at room temperature. Finally, the tissue was stained with DAB (ZLI-9019, ZSGB-BIO, China) and haematoxylin, dehydrated, cleared, and mounted. The samples were photographed and analysed using an optical microscope.

Animal experiments

BALB/c male nude mice (approximately 6 weeks old) were purchased from Guangxi Medical University and maintained in a specific pathogen-free facility. The appropriate temperature, humidity, and 12-hour light/12-hour dark cycle were maintained. All the animal studies were approved by the Animal Care and Use Committee of the First Affiliated Hospital of Guangxi Medical University. All studies were conducted in accordance with the Guide for the Care and Use of Laboratory Animals. The prepared cells were inoculated subcutaneously into

nude mice. Four weeks later, the subcutaneous tumours were harvested from the mice, the tumour volumes were measured, and the tumours were weighed. Finally, the tumour tissues were fixed or stored at −80 °C for subsequent experiments.

Statistical analysis

All the data are presented as the means ± S.D.s. Differences between two groups were analysed via unpaired Student's t tests. Comparisons among multiple groups were performed by means of one-way analysis of variance (ANOVA). *P* values less than 0.05 were considered to indicate statistical significance. All the tests were repeated at least three times (*: $P < 0.05$, **: $P < 0.01$, and ***: $P < 0.001$).

Results

Bioinformatics analysis revealed that lnc-POTEM-4:14 was correlated with the malignant progression of HCC

To elucidate the associations between lncRNAs and the development of liver cancer, we analysed the differentially expressed lncRNAs (DElncRNAs) in liver cancer and adjacent tissues using two GEO datasets (GSE166705 and GSE115018). These RNA-seq datasets were annotated separately and combined with batch correction and standardization. Boxplots indicated that the quality of the datasets after batch correction and standardization met the requirements for subsequent bioinformatics analysis (Supplementary Fig. 1A and B). A heatmap of differential RNA expression revealed 2237 differentially expressed RNAs with *P* values < *0.05* and | log2FC | > 1 (Fig. 1A), among which 1447 were upregulated and 790 were downregulated (Supplementary Fig. 1C), and the comprehensive datasets detailed in Supplementary Table (1) There were 560 differentially expressed lncRNAs, of which 344 were upregulated and 216 were downregulated (Fig. 1B), all detected lncRNAs are listed in Supplementary Table (2) To analyse the lncRNAs associated with HCC, WGCNA was employed to construct a coexpression network and explore the coexpression modules of lncRNAs associated with HCC. When the scale-free topological index reached 0.85, the optimal soft threshold power was set to 10 (Supplementary Fig. 1D), and then modules were created using the topological overlap matrix. All the lncRNAs could be divided into 10 modules, and the ones most highly correlated with HCC (blue and green modules) were used for further screening and analysis (Fig. 1C and Supplementary Fig. 1E).

For further screening, LASSO and SVM-RFE models were constructed for candidate DElncRNAs in these modules that met the significance criteria. The intersection of the results from the two models was taken. In MEblue, 10 feature lncRNAs were identified by LASSO and 10 by SVM-RFE (Fig. S1 H and I), and 5 common feature lncRNAs were identified (Supplementary Fig. 1F). In MEgreen, 6 feature lncRNAs were identified by LASSO and 2 by SVM-RFE (Supplementary Fig. 1J and K), and 1 common feature lncRNA was identified (Supplementary Fig. 1G). Finally, the results from the two modules were combined to obtain 6 transcripts, and duplicates were removed, five feature lncRNAs were found. ROC curves were used to evaluate the testing efficiency of characteristic lncRNA sets. In the training set, the AUC indices of AP000525, lnc-POTEM-4:14, ST8SIA6-AS, TEX41 and AC239798 were 0.800, 0.826, 0.678, 0.769 and 0.977 (Fig. 1D), respectively. The AUC index of the characteristic lncRNA set was 0.990 (Fig. 1E). These results indicate that the lncRNA set can distinguish HCC from the control set in both the training set and the verification set (Fig. 1F and G).

Among the characteristic lncRNAs, AP000525, lnc-POTEM-4:14 and AC239798 were highly correlated with liver cancer ($P < 0.001$), and their expression levels are shown by box diagrams (Fig. 1H). The AUC index and expression level of lnc-POTEM-4:14 were the highest among these three lncRNAs. The survival analysis results further revealed that the characteristic lncRNA lnc-POTEM-4:14 was correlated with the malignant progression of HCC (Fig. 1I). These data suggest that lnc-POTEM-4:14lnc-POTEM-4:14 may be associated with the progression of HCC patients.

Lnc-POTEM-4:14 is upregulated in HCC and promotes the proliferation of HCC cells

According to the LNCipedia database (version 5.2), lnc-POTEM-4:14 (alternative transcript names: OTTHUMT00000317886.1; NONHSAT035484; ENST00000427798.1; AL589743.1-002) is a lncRNA with a length of 990 bp (https://lncipedia.org/db/transcript/lnc-POTEM-4:14). LncRNA expression is different in various HCC lines due to different genetic background, so the expression of lnc-POTEM-4:14 in liver cancer tissues was tested using qPCR. The results revealed that lnc-POTEM-4:14 was significantly upregulated in tumour tissues (Fig. 2A), and the expression of lnc-POTEM-4:14 in different liver cancer cells was also tested (Fig. 2B). RNA fluorescence in situ hybridization (FISH) confirmed that lnc-POTEM-4:14 is localized in the nucleus (Fig. 2C). Nucleocytoplasmic separation demonstrated that lnc-POTEM-4:14 was predominantly located in the nucleus of Huh-7 cells (Fig. 2D). According to previous studies, antisense oligonucleotides (ASOs) are more effective than siRNAs for knocking down predominantly nucleus-localized lncRNAs[28]. Therefore, we utilized ASO to knock down lnc-POTEM-4:14 in Huh-7 cell lines, which presented relatively high expression levels (Fig. 2B). Conversely, we overexpressed lnc-POTEM-4:14 in MHCC-97 H cells, which had relatively low expression levels (Fig. 2B). The effects of lncRNA knockdown and overexpression were detected by qPCR (Fig. 2E and F). To evaluate the impact of lnc-POTEM-4:14 on the proliferation of HCC cells, we conducted an EdU proliferation experiment. Compared with the NC group, the percentage of cells in the S phase was significantly lower in the ASO-treated group, whereas the opposite effect was detected in the overexpression group (Fig. 2G-H). Colony formation and CCK8 assays further demonstrated that, ASO treatment significantly reduced cell proliferation compared to that in the NC group, while overexpression had the opposite effect (Fig. 2I-N). Taken together, these results indicate that lnc-POTEM-4:14 is located in the cell nucleus and is upregulated in HCC and promotes the proliferation of HCC cells.

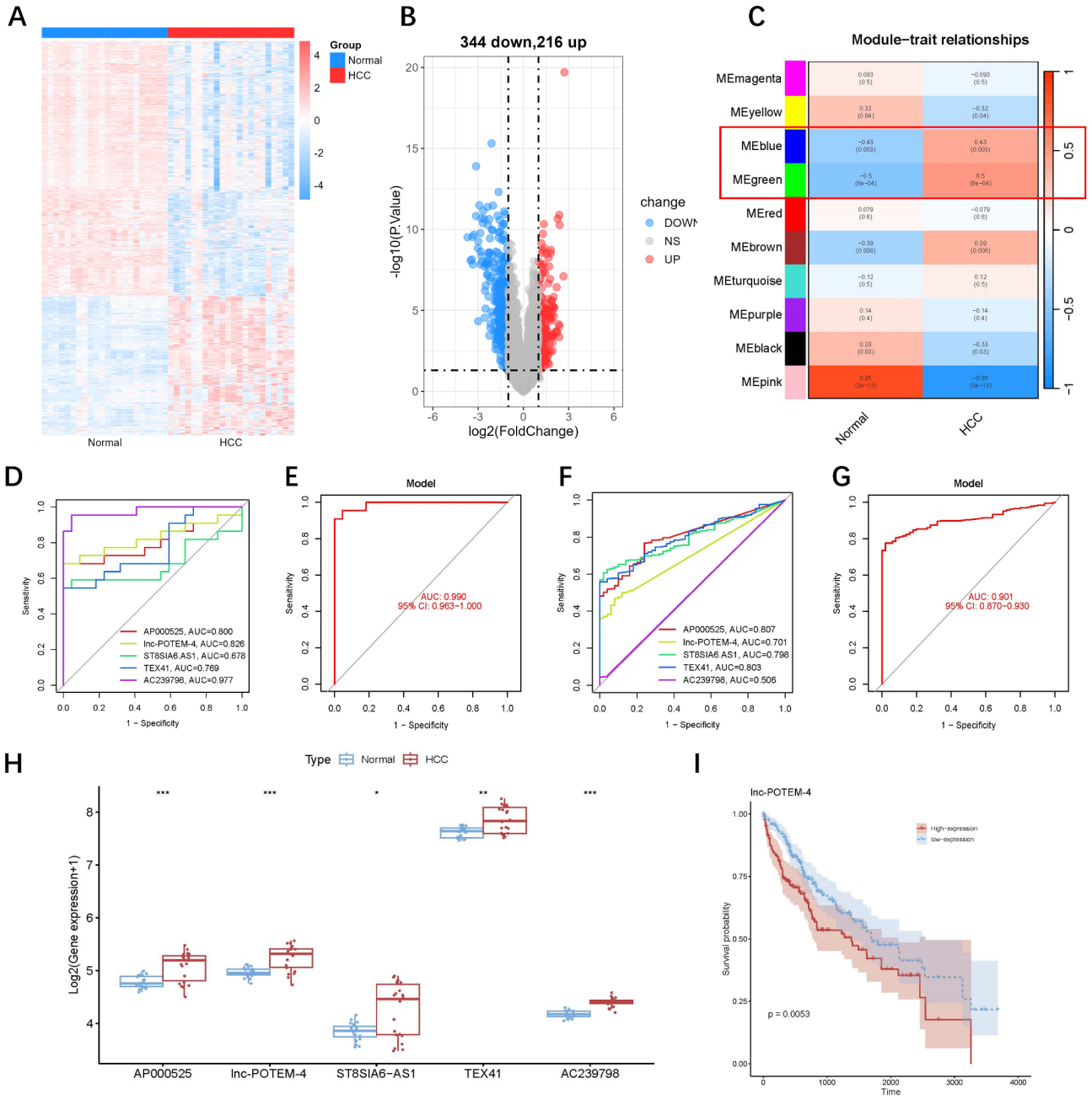

Fig. 1. Bioinformatics analysis revealed that lnc-POTEM-4:14 was correlated with the malignant progression of HCC. (**A**) Heatmap of differential RNA expression between the HCC group and the control group. (**B**) Volcano plot of differentially expressed lncRNAs. (**C**) Heatmap of module–HCC correlation coefficients. (**D**) ROC curve of signature lncRNAs (training set). (**E**) ROC curve of the signature lncRNA set (training set). (**F**) ROC curve of the signature lncRNA set (validation set). (**G**) ROC curve of the signature lncRNA set (validation set). (**H**) Expression levels of 5 characteristic lncRNAs in merged GEO datasets. (**I**) Survival curves of the individual signature lncRNA lnc-POTEM-4:14. All values are expressed as the means ± SDs. $^{*}P < 0.05$, $^{**}P < 0.01$, $^{***}P < 0.001$.

Lnc-POTEM-4:14 regulates the cell cycle and apoptosis of HCC cells in vitro

Flow cytometry was used to evaluate the impact of lnc-POTEM-4:14 on the cell cycle of HCC cells. The results showed that the cell cycle in the ASO group was arrested in the G1/G0 phase, whereas cell cycle arrest was not observed in the overexpression group (Fig. 3A and B). In addition, cell apoptosis analysis indicated that ASO treatment significantly increased HCC cell apoptosis (Fig. 3C). The WB results showed that compared to those in the NC group, the protein expression levels of CDK2 and Cyclin E1 were significantly lower after ASO treatment (Fig. 3D). The WB results revealed that the protein expression levels of BAX and c-CASP3 were significantly increased in the ASO group, whereas the protein expression level of BCL2 was significantly decreased. The

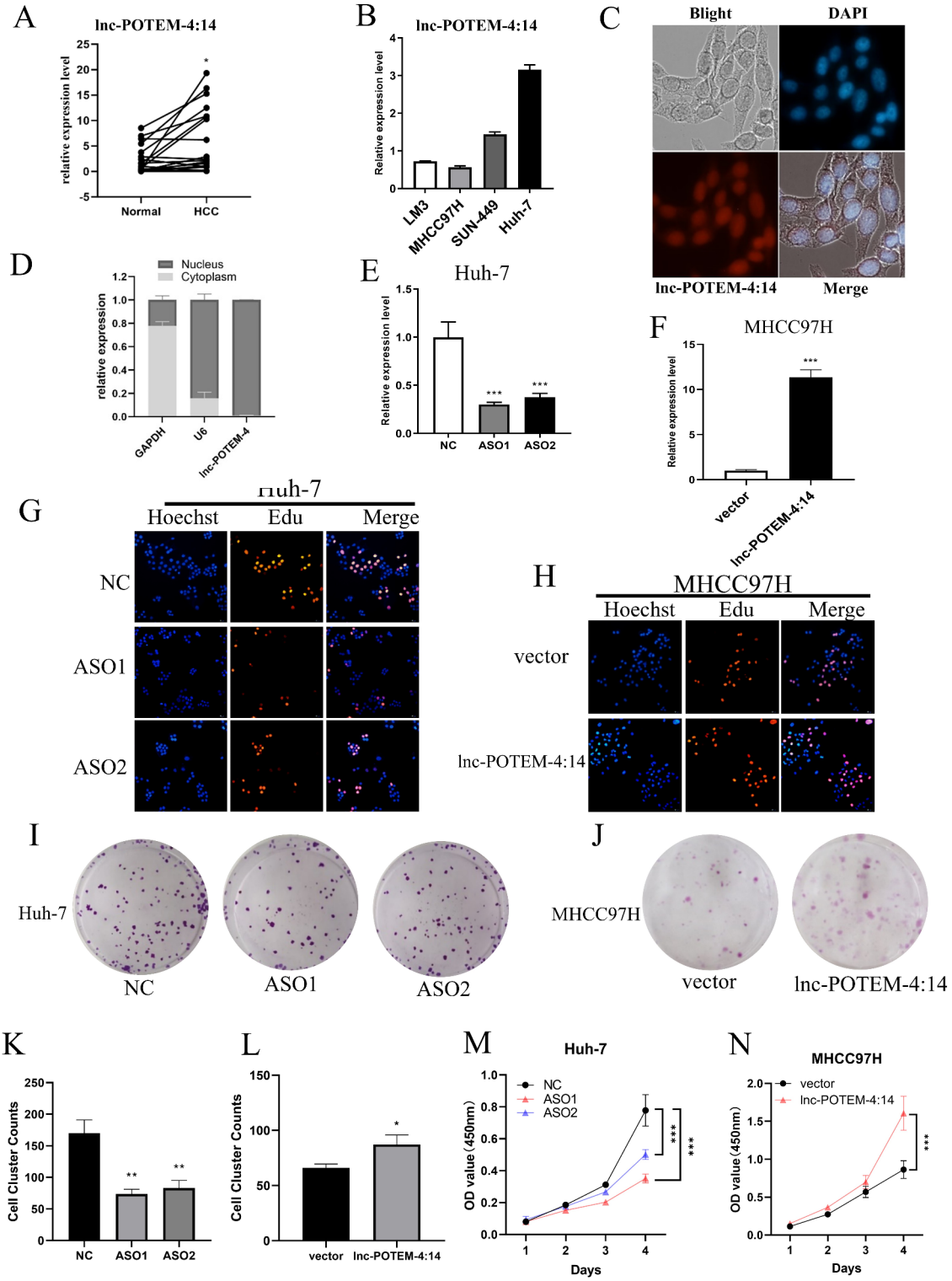

Fig. 2. Lnc-POTEM-4:14 is located in the cell nucleus and is associated with HCC proliferation in vitro. (**A**) qPCR analysis of lnc-POTEM-4:14 expression between clinical HCC and adjacent normal tissues. (**B**) qPCR analysis of lnc-POTEM-4:14 expression in different HCC cell lines. (**C**) Nuclear–cytoplasmic segregation of lnc-POTEM-4:14 in Huh-7 cells. (**D**) FISH of lnc-POTEM-4:14 in Huh-7 cells. Scale bar, 20 μm. (**E**–**F**) qPCR analysis of Huh-7 cells treated with ASO and MHCC97H cells overexpressing lnc-POTEM-4:14. (**E**) EdU analysis of proliferative ability. (**I**–**L**) Colony formation assay results and their statistical graph. (**M**–**N**) CCK-8 assay results. Scale bar, 200 μm. All values are expressed as the means ± SDs (*: $P < 0.05$, **: $P < 0.005$, ***: $P < 0.001$).

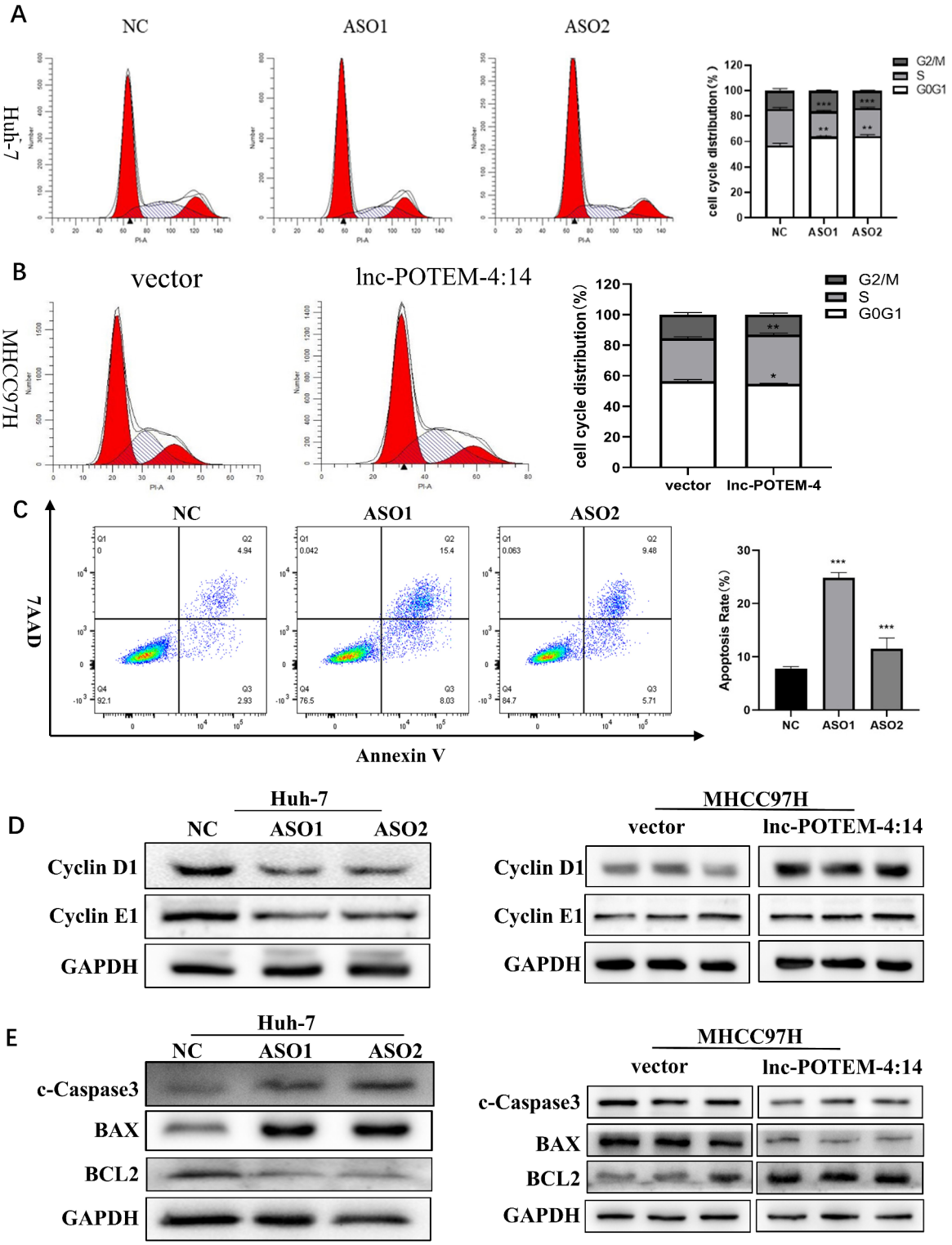

Fig. 3. Lnc-POTEM-4:14 affects HCC cell cycle progression and apoptosis. (**A**–**B**) Flow cytometry analysis of the effect of lnc-POTEM-4:14 on the cell cycle. (**C**) Flow cytometry analysis of the effect of lnc-POTEM-4:14 on apoptosis. (**D**–**E**) Changes in the expression levels of cell cycle- and apoptosis-related proteins after lnc-POTEM-4:14 intervention. The original blots are presented in Supplementary Figs. 8 and 9. The data shown are the means ± SDs ($n = 3$).

overexpression group showed the opposite trend with respect to the NC group (Fig. 3E). These results show that lnc-POTEM-4:14 regulates the cell cycle and apoptosis of HCC cells in vitro.

Lnc-POTEM-4:14 regulates the growth of HCC tumours in vivo

To further confirm the role of lnc-POTEM-4:14 in vivo, we established a subcutaneous tumour-bearing model in nude mice. Knockdown of lnc-POTEM-4:14 resulted in delayed liver cancer growth, as reflected by tumour size, weight (Fig. 4A and B), and Ki67 staining (Fig. 4C). Additionally, we investigated the oncogenic effects of lnc-POTEM-4:14 overexpression. The results indicated that the overexpression of lnc-POTEM-4:14 accelerated tumour growth.

FOXK1 is the RBP of lnc-POTEM-4:14

To further elucidate the underlying mechanism, we identified Forkhead box k1 (FOXK1) as an RBP (RNA-binding protein) that acts as a transcription factor (TF) among the proteins bound to lnc-POTEM-4:14. This identification was achieved by integrating data from TF databases (AnimalTFDB, TFSyntax) with mass

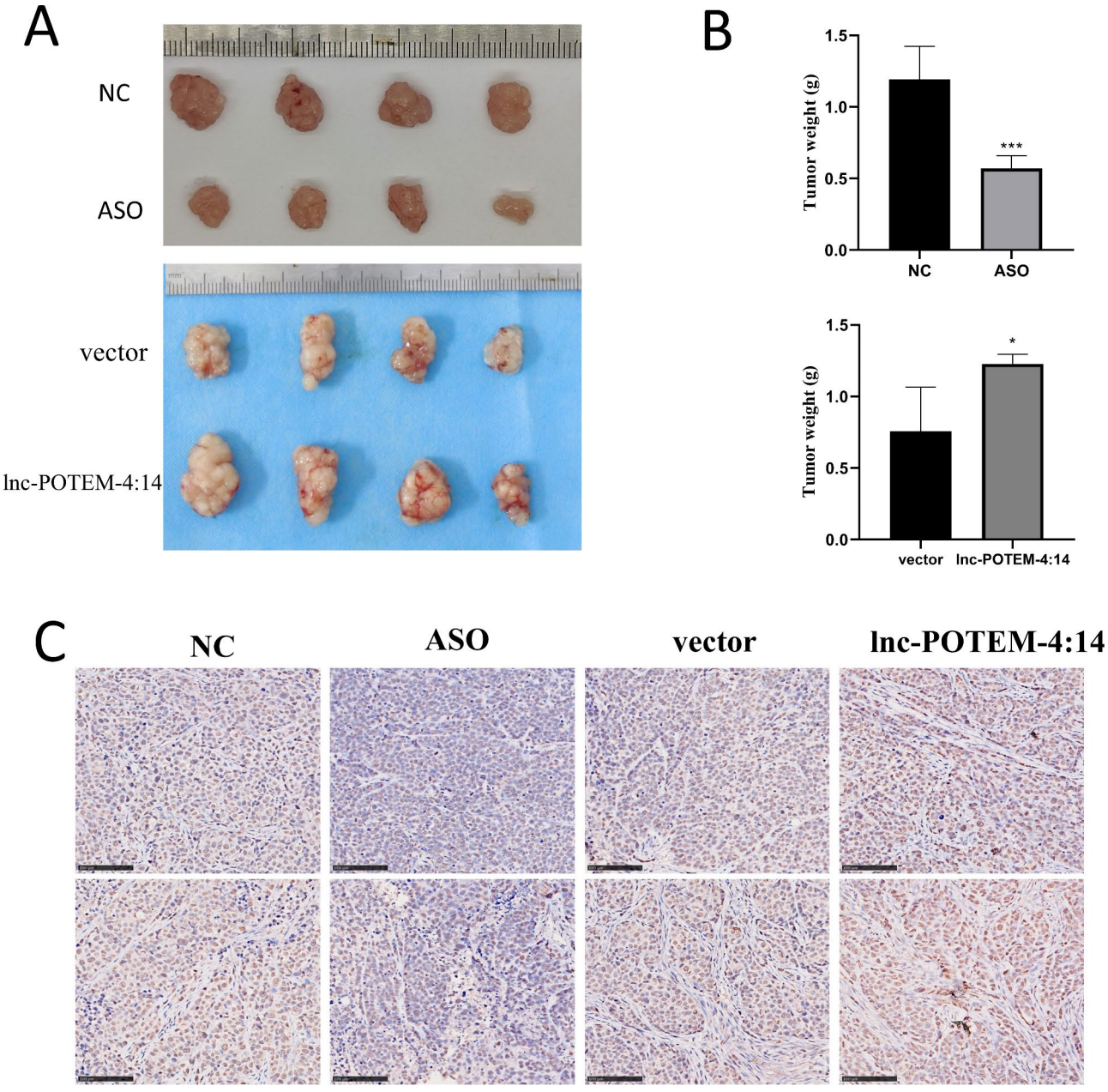

Fig. 4. Lnc-POTEM-4:14 affects the growth of HCC in vivo. (**A**) Images of tumours formed from Huh-7 and MHCC97H cells that were subcutaneously injected with lnc-POTEM-4:14. (**B**) Tumour weight. (**C**) Ki67 immunohistochemical staining results. Scale bar, 100 μm. All values are expressed as the means ± SDs (*: $P < 0.05$, **: $P < 0.005$, ***: $P < 0.001$).

spectrometry analysis of RNA pulldown products (Fig. 5A and B). We subsequently confirmed their interaction through RNA immunoprecipitation (RIP) experiments (Fig. 5C). TCGA database analysis revealed that FOXK1 is highly expressed in HCC (Fig. 5D). Overall survival analysis revealed that patients with high expression of FOXK1 had poor prognoses, according to the TCGA database (Fig. 5E). qPCR results revealed that the expression level of FOXK1 was greater in clinical HCC samples than in normal samples (Fig. 5F). qPCR and WB results suggested that the knockdown/overexpression of lnc-POTEM-4:14 reduced/increased both the mRNA and protein expression of FOXK1 (Fig. 5G-I). These findings indicated that lnc-POTEM-4:14 is associated with FOXK1 in liver cancer cells, specifically in its transcriptional regulatory role.

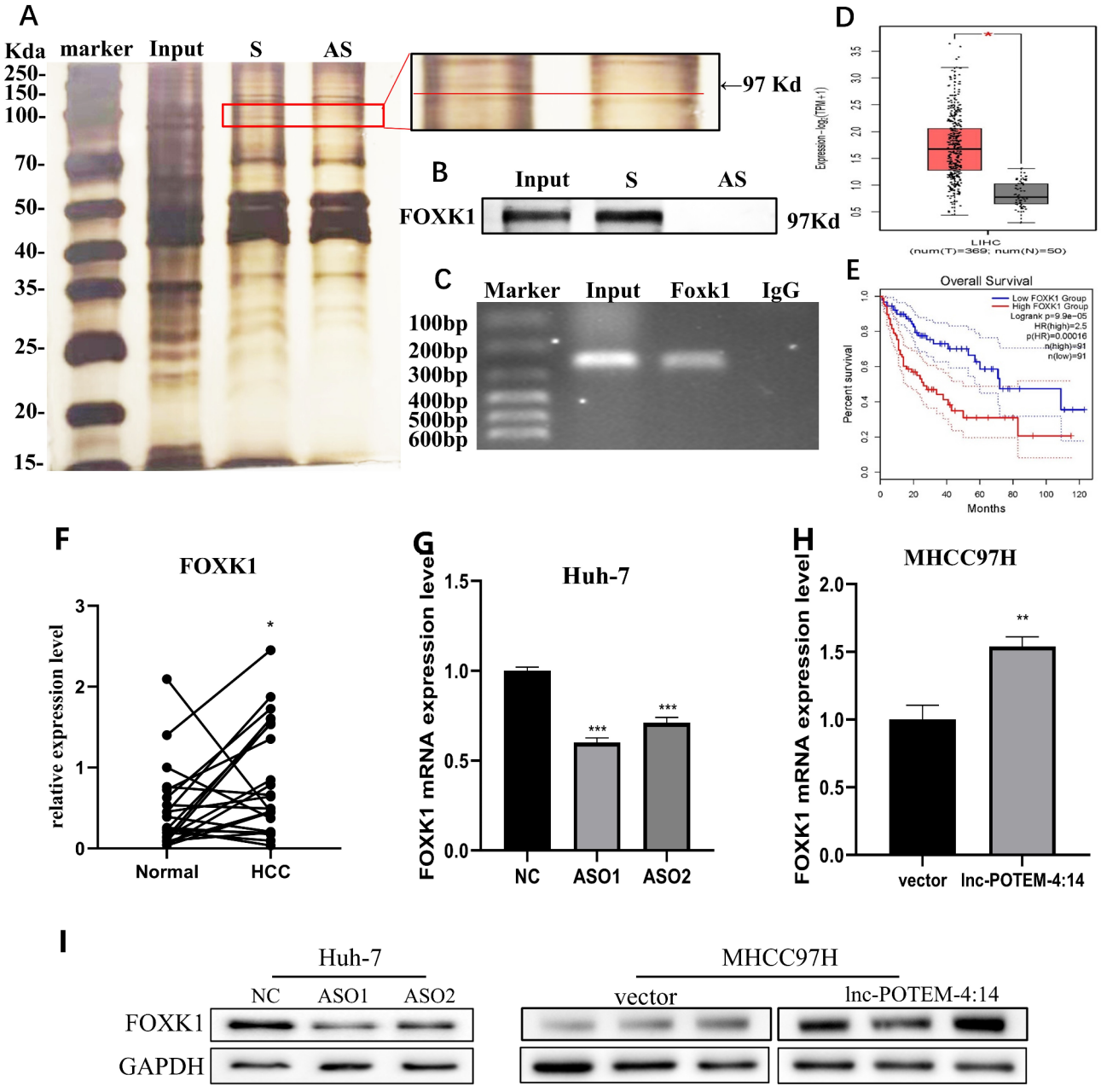

Fig. 5. FOXK1 is the RBP of lnc-POTEM-4:14. (**A**) SDS-PAGE gel silver staining results of the RNA pull-down products. (**B**) WB results of the RNA pull-down products. (**C**) Electrophoresis results of the RIP products. (**D**) TCGA database analysis revealed that FOXK1 is highly expressed in HCC. (**E**) TCGA database analysis revealed the effect of FOXK1 on the survival curve of patients with HCC. (**F**) Expression levels of FOXK1 in clinical samples ($n = 20$). (**G**) FOXK1 mRNA expression in lnc-POTEM-4:14-knockdown Huh-7 cells. (**H**) FOXK1 mRNA expression in lnc-POTEM-4:14-overexpressing MHCC97H cells. (**I**) Disruption of FOXK1 protein expression in cell lines subjected to lnc-POTEM-4:14 interference; original blots are presented in Supplementary Fig. 10. The data shown are the means ± SDs ($n = 3$), *: $P < 0.05$, **: $P < 0.01$, ***: $P < 0.001$.

Lnc-POTEM-4:14 may affect the malignancy of HCC through the FOXK1/TAB1 axis

To explore the mechanism by which lnc-POTEM-4:14 regulates downstream signalling pathways, RNA-seq was performed on the NC group and the ASO group. The boxplot and PCA results indicated that the data quality and intragroup consistency of the RNA-seq dataset were satisfactory for subsequent bioinformatics analysis (Supplementary Fig. 5A and B). Furthermore, we observed significant enrichment of the MAPK pathway by KEGG enrichment analysis (Fig. 6A) Wiki Pathways enrichment analysis also showed MAPK pathway was a major enrichment pathway (Supplementary Fig. 6). Correlation analysis of FOXK1 with the gene set of the MAPK signalling pathway revealed that FOXK11 is highly correlated with the MAPK pathway (Supplementary Fig. 7). The predicted FOXK1 target genes in the JASPAR database, FOXK1-related genes in the TCGA database and differentially expressed genes in the MAPK signalling pathway were combined to screen FOXK1 target genes, and five possible target genes were obtained (Fig. 6B). Interestingly, transforming growth factor-β-activated kinase 1 binding protein 1 (TAB1) was the only gene whose expression was downregulated, and its gene expression level was in line with expectations (Supplementary Table 5). Further analysis revealed that nemo-like kinase (NLK), which is a downstream pathway gene of TAB1, was an important differentially expressed gene in the MAPK pathway. qPCR and WB confirmed that ASO treatment reduced the expression of TAB1 and NLK in the MAPK pathway (Fig. 6C and D). We confirmed their binding via ChIP-qPCR, and the results showed that FOXK1 can bind to the promoter region of TAB1 (Fig. 6E) but not NLK (Fig. 6F), which is consistent with previous results (Fig. 6B), indicating that FOXK1 is a transcription factor of TAB1. ASO-mediated knockdown of lnc-POTEM-4:14 decreased the expression of TAB1 and NLK (Fig. 6G). The results of rescue experiments demonstrated that restoring FOXK1 expression could partly rescue the reduction in TAB1 and NLK expression caused by ASO treatment (Fig. 6H), as well as the effects on cell cycle-related proteins and apoptosis-related proteins (Fig. 6I). These results illustrate that the lncRNA lnc-POTEM-4:14 regulates the expression of TAB1 and its downstream NLK by binding to FOXK1, thereby affecting the progression of liver cancer.

Discussion

HCC remains one of the most widespread and fatal cancers and significantly impacts the quality of life and safety of individuals worldwide[29]. In recent years, numerous studies have demonstrated that lncRNAs are involved in the development and progression of liver cancer and affect the prognosis of patients with liver cancer[8]. By analysing GEO datasets (GSE166705 and GSE115018), we identified a previously unstudied lncRNA, lnc-POTEM-4:14. We observed that lnc-POTEM-4:14 is highly expressed in HCC and is closely associated with the cell cycle signalling pathway. On the basis of these findings, we hypothesize that lnc-POTEM-4:14 promotes the progression of HCC and may impact prognosis.

Our functional experiments conclusively revealed that lnc-POTEM-4:14 promotes the proliferation of HCC cells while suppressing apoptosis. Mechanistically, we hypothesize that lnc-POTEM-4:14 binds to FOXK1, increasing FOXK1 expression. FOXK1 is a member of the Forkhead box transcription factor superfamily. Studies have shown that FOXK1 can induce the proliferation, migration, and invasion of various cancer cells[30], and FOXK1 knockdown significantly inhibits the malignant behaviour of liver cancer cells[25]. FOXK1 not only directly participates in the initiation and progression of tumours but is also regulated by various lncRNAs, such as SNHG1[26] and PART1[31]. Interestingly, FOXK1 is not a typical RBP. FOXK1 consists of 733 amino acids[32] and contains two highly conserved domains, a Forkhead winged helix–turn–helix DNA binding domain (FOX) and a Forkhead-associated domain (FHA). FOX mediates its binding to DNA, and FHA mediates its interaction with other proteins[24]. In addition, it contains a Swi-independent 3b-interacting domain (SID) in the N-terminus, and amino acids 95–420 mediate its interaction with other regions of the molecule[33–36]. FOXK1 does not contain a typical RNA binding domain, but we found evidence in the RPIseq database (http://pridb.gdcb.iastate.edu/RPISeq/index.html) that the lncRNA lnc-POTEM-4:14 might interact with FOXK1. This finding is consistent with our results. We speculate that the lncRNA lnc-POTEM-4:14 may also interact with FOXK1 through other proteins.

Our data demonstrate that FOXK1, as a transcription factor, binds directly to the promoter region of TAB1, thereby promoting its transcription and translation. TAB1 is a member of the MAPK kinase family and has been identified as a potential tumour suppressor whose activation can promote the activation of the MAPK signalling pathway[37]. The MAPK signalling pathway is one of the crucial pathways in the eukaryotic signal transduction network[38]. It can amplify cellular signals through a three-tiered kinase cascade and serves as a key signalling pathway for cell proliferation, differentiation, apoptosis, and stress responses under both normal and pathological conditions[39,40]. The MAPK pathway comprises three classical pathways involving three key factors: ERK, c-Jun NH2-terminal kinase (JNK), and p38[41,42]. Studies have shown that TAB1 can activate JNK and p38 by activating TAK1 as a scaffold protein and can also directly induce autophosphorylation of p38α through an atypical mode[43].

The atypical activation of the p38 signal induced by TAB1 is initiated under pathological conditions, including cancer, viral infections, and inflammation. TAB1-p38α can induce necrosis[44] and apoptosis[45] in cardiomyocytes. This contradicts our functional experimental results, and after an extensive literature review and analysis of the sequencing results, we ultimately identified NLK as a potential downstream target. NLK is a member of the extracellular-signal-regulated kinases/microtubule-associated protein kinases and cyclin-directed kinases. Upon activation by FOXK1, TAK1 can inhibit the β-catenin/TCF complex through NLK, leading to cell cycle arrest in the G1 phase and the suppression of cell proliferation[46,47]. We hypothesize that FOXK1 regulates the development and progression of liver cancer by activating the TAB1/pTAK1/NLK axis, which was confirmed by the qPCR and WB results.

Many lncRNAs have been reported to regulate the stability of their binding proteins[48,49], It is not clear whether lnc-POTEM-4-14 affects the stability of FOXK1 protein. In this study, our investigation into the mechanism of action of lnc-POTEM-4-14 revealed its ability to bind to the FOXK1 protein. This interaction promotes the

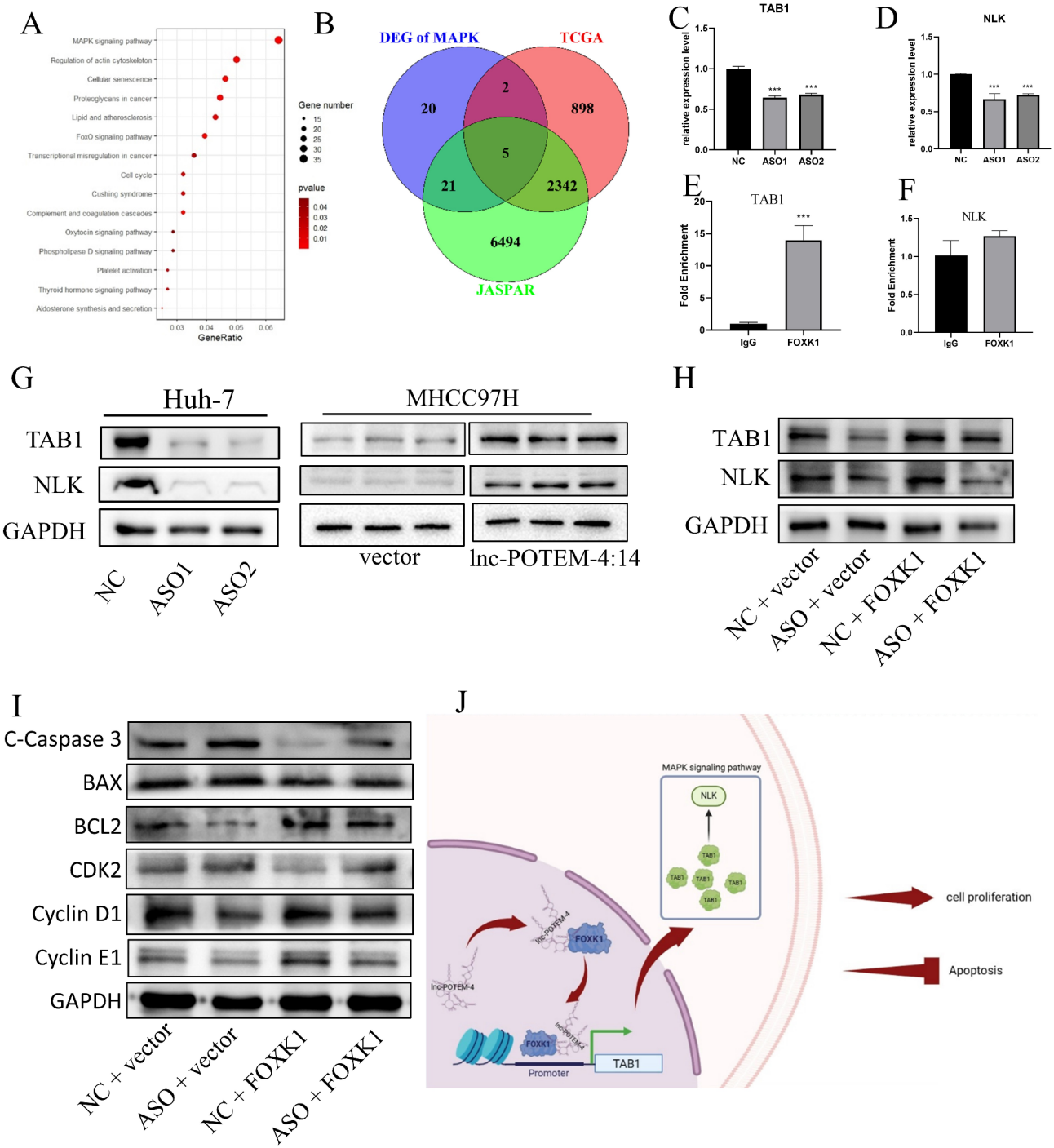

Fig. 6. Lnc-POTEM-4:14 may affect the malignancy of HCC through the FOXK1/TAB1 axis. (**A**) KEGG analysis after lnc-POTEM-4:14 knockdown. (**B**) Prediction of FOXK1 target genes. (**C**–**D**) qPCR analysis of TAB1 and NLK after lnc-POTEM-4:14 intervention. (**E**–**F**) Chip-qPCR was used to examine the ability of FOXK1 to bind to the promoter regions of TAB1 and NLK. (**G**) WB analysis of TAB1 and NLK after lnc-POTEM-4:14 intervention; original blots are presented in Supplementary Fig. 11. (**H**) WB analysis of TAB1 and NLK after FOXK1 rescue; original blots are presented in Supplementary Fig. 12. (**I**) WB analysis of cell cycle and apoptosis proteins after FOXK1 rescue; original blots are presented in Supplementary Fig. 13. (**J**) Graphical abstract showing that lnc-POTEM-4:14 regulates the progression of HCC. The data shown are the means ± SDs ($n = 3$), *: $P < 0.05$, **: $P < 0.01$, ***: $P < 0.001$.

recruitment of FOXK1 to the promoter region of the TAB1 gene, thereby initiating its transcriptional activation. Although lnc-POTEM-4-14 knockdown results in the decrease of FOXK1 protein expression, overexpression of lnc-POTEM-4-14 results in the increase of FOXK1. However, knockdown and overexpression of lnc-POTEM-4-14 also caused changes in FOXK1 mRNA content, so more studies are needed to determine the effect of lnc-POTEM-4-14 on the stability of FOXK1 protein. Then, we propose that lnc-POTEM-4-14 interacts with FOXK1 to facilitate its binding to TAB1, thereby advancing our understanding of the associated pathways. Although the lnc-POTEM-4-14/FOXK1/TAB1 axis has been identified as a potential therapeutic target for HCC, no inhibitors for lnc-POTEM-4-14 or FOXK1 have been reported thus far. Consequently, we have initiated preliminary screening of small-molecule inhibitors targeting this axis to evaluate their potential for drug development in the clinical management of HCC.

In summary, our current data imply that lnc-POTEM-4:14 facilitates the malignant behaviour and poor prognosis of HCC in vitro and in vivo. lnc-POTEM-4:14 influences the proliferation and apoptosis of liver carcinoma cells by interfering with the MAPK signalling pathway and cell cycle progression through the FOXK1/TAB1/NLK axis. The identification of this molecular mechanism not only enhances our understanding of HCC pathogenesis but also highlights lnc-POTEM-4:14 as a potential therapeutic target for the treatment of this aggressive malignancy (Fig. 6J).

Data availability

Data will be available upon reasonable requests from the corresponding author.

Received: 13 November 2024; Accepted: 3 March 2025
Published online: 05 March 2025

References

1. Yang, J. D. et al. A global view of hepatocellular carcinoma: Trends, risk, prevention and management. *Nat. Rev. Gastroenterol. Hepatol.* **16**(10), 589–604 (2019).
2. Villanueva, A. Hepatocellular carcinoma. *N. Engl. J. Med.* **380**(15), 1450–1462 (2019).
3. Sarfaraz, N., Somarowthu, S. & Bouchard, M. J. The interplay of long noncoding RNAs and hepatitis B virus. *J. Med. Virol.* **95**(1), e28058 (2023).
4. Shimada, S. et al. Comprehensive molecular and immunological characterization of hepatocellular carcinoma. *EBioMedicine* **40**, 457–470 (2019).
5. Patraquim, P., Magny, E. G., Pueyo, J. I., Platero, A. I. & Couso, J. P. Translation and natural selection of micropeptides from long non-canonical RNAs. *Nat. Commun.* **13**(1). (2022).
6. Zhang, Y., Jia, C. & Kwoh, C. K. Predicting the interaction biomolecule types for LncRNA: an ensemble deep learning approach. *Brief. Bioinform.* **22**(4). (2021).
7. Qian, X., Zhao, J., Yeung, P. Y., Zhang, Q. C. & Kwok, C. K. Revealing LncRNA structures and interactions by sequencing-based approaches. *Trends Biochem. Sci.* **44**(1), 33–52 (2019).
8. Huang, Z., Zhou, J. K., Peng, Y., He, W. & Huang, C. The role of long noncoding RNAs in hepatocellular carcinoma. *Mol. Cancer* **19**(1), 77 (2020).
9. Li, C., Yang, J., Liu, C., Wang, X. & Zhang, L. Long non-coding RNAs in hepatocellular carcinoma: Ordering of the complicated LncRNA regulatory network and novel strategies for HCC clinical diagnosis and treatment. *Pharmacol. Res.* **158**, 104848 (2020).
10. Cao, P. et al. Emerging roles and potential clinical applications of noncoding RNAs in hepatocellular carcinoma. *Sem. Cancer Biol.* **75**, 136–152 (2021).
11. Ho, J. J. D., Man, J. H. S., Schatz, J. H. & Marsden, P. A. Translational remodeling by RNA-binding proteins and noncoding RNAs. *Wiley Interdisciplinary Reviews RNA* **12**(5), e1647 (2021).
12. Cabili, M. N. et al. Localization and abundance analysis of human LncRNAs at single-cell and single-molecule resolution. *Genome Biol.* **16**(1), 20 (2015).
13. Engreitz, J. M. et al. The Xist LncRNA exploits three-dimensional genome architecture to spread across the X chromosome. *Sci. (New York NY)* **341**(6147), 1237973 (2013).
14. Kretz, M. et al. Control of somatic tissue differentiation by the long non-coding RNA TINCR. *Nature* **493**(7431), 231–235 (2013).
15. Guo, C. J., Xu, G. & Chen, L. L. Mechanisms of long noncoding RNA nuclear retention. *Trends Biochem. Sci.* **45**(11), 947–960 (2020).
16. Engreitz, J. M. et al. Local regulation of gene expression by LncRNA promoters, transcription and splicing. *Nature* **539**(7629), 452–455 (2016).
17. Xiang, J. F. et al. Human colorectal cancer-specific - lncRNA regulates long-range chromatin interactions at the locus. *Cell. Res.* **24**(5), 513–531 (2014).
18. Hu, W. L. et al. GUARDIN is a p53-responsive long non-coding RNA that is essential for genomic stability. *Nat. Cell. Biol.* **20**(4), 492– (2018).
19. Yang, L. et al. Long non-coding RNA HOTAIR promotes exosome secretion by regulating RAB35 and SNAP23 in hepatocellular carcinoma. *Mol. Cancer* **18** (2019).
20. Huang, Y. et al. Large scale RNA-binding proteins/lncrnas interaction analysis to uncover LncRNA nuclear localization mechanisms. *Brief. Bioinform.* **22**(6). (2021).
21. Hentze, M. W., Castello, A., Schwarzl, T. & Preiss, T. A brave new world of RNA-binding proteins. *Nat. Rev. Mol. Cell Biol.* **19**(5), 327–341 (2018).
22. Søndergaard, J. N. et al. CCT3-LINC00326 axis regulates hepatocarcinogenic lipid metabolism. *Gut* **71**(10), 2081–2092 (2022).
23. Katoh, M. & Katoh, M. Human FOX gene family (Review). *Int. J. Oncol.* **25**(5), 1495–1500 (2004).
24. Liu, Y. et al. FOXK transcription factors: Regulation and critical role in cancer. *Cancer Lett.* **458**, 1–12 (2019).
25. Li, P. et al. Knockdown of FOXK1 inhibited the proliferation, migration and invasion in hepatocellular carcinoma cells. *Biomed. Pharmacother. Biomed. Pharmacother.* **92**, 270–276 (2017).
26. Meng, F. et al. SNHG1 knockdown upregulates miR-376a and downregulates FOXK1/Snail axis to prevent tumor growth and metastasis in HCC. *Mol. Therapy Oncolytics.* **21**, 264–277 (2021).
27. Li, Z. et al. Transcriptome sequencing and metabolome analysis reveal the metabolic reprogramming of partial hepatectomy and extended hepatectomy. *BMC Genom.* **24**(1), 532 (2023).
28. Lennox, K. A. & Behlke, M. A. Cellular localization of long non-coding RNAs affects Silencing by RNAi more than by antisense oligonucleotides. *Nucleic Acids Res.* **44**(2), 863–877 (2016).
29. Llovet, J. M. et al. Molecular pathogenesis and systemic therapies for hepatocellular carcinoma. *Nat. cancer* **3**(4), 386–401 (2022).

30. Peng, Y. et al. Direct regulation of FOXK1 by C-jun promotes proliferation, invasion and metastasis in gastric cancer cells. *Cell. Death Dis.* **7**(11), e2480 (2016).
31. Li, B., Lou, G., Zhang, J., Cao, N. & Yu, X. Repression of LncRNA PART1 attenuates ovarian cancer cell viability, migration and invasion through the miR-503-5p/FOXK1 axis. *BMC Cancer* **22**(1), 124 (2022).
32. Huang, J. T. & Lee, V. Identification and characterization of a novel human FOXK1 gene in Silico. *Int. J. Oncol.* **25**(3), 751–757 (2004).
33. Shi, X., Bowlin, K. M. & Garry, D. J. Fhl2 interacts with Foxk1 and corepresses Foxo4 activity in myogenic progenitors. *Stem Cells (Dayton Ohio)* **28**(3), 462–469 (2010).
34. Shi, X., Seldin, D. C. & Garry, D. J. Foxk1 recruits the Sds3 complex and represses gene expression in myogenic progenitors. *Biochem. J.* **446**(3), 349–357 (2012).
35. Shi, X. & Garry, D. J. Sin3 interacts with Foxk1 and regulates myogenic progenitors. *Mol. Cell. Biochem.* **366**(1–2), 251–258 (2012).
36. Shi, X. et al. Foxk1 promotes cell proliferation and represses myogenic differentiation by regulating Foxo4 and Mef2. *J. Cell Sci.* **125**(Pt 22), 5329–5337 (2012).
37. Kong, Q. W. et al. Tongguanteng injection reverses Paclitaxel resistance via upregulation of table 1 expression in ovarian cancer in vitro and in vivo. *J. Ethnopharmacol.* **300**, 115728 (2023).
38. Johnson, G. L. & Lapadat, R. Mitogen-activated protein kinase pathways mediated by ERK, JNK, and p38 protein kinases. *Sci. (New York NY)* **298**(5600), 1911–1912 (2002).
39. Cargnello, M. & Roux, P. P. Activation and function of the MAPKs and their substrates, the MAPK-activated protein kinases. *Microbiol. Mol. Biol. Rev. MMBR* **75**(1), 50–83 (2011).
40. Bahar, M. E., Kim, H. J. & Kim, D. R. Targeting the RAS/RAF/MAPK pathway for cancer therapy: From mechanism to clinical studies. *Signal. Transduct. Target. Ther.* **8**(1), 455 (2023).
41. Phan, T., Zhang, X. H., Rosen, S. & Melstrom, L. G. P38 kinase in Gastrointestinal cancers. *Cancer Gene Ther.* **30**(9), 1181–1189 (2023).
42. Aashaq, S., Batool, A. & Andrabi, K. I. TAK1 mediates convergence of cellular signals for death and survival. *Apoptosis: Int. J. Program. Cell. Death* **24**(1–2), 3–20 (2019).
43. Burton, J. C., Antoniades, W., Okalova, J., Roos, M. M. & Grimsey, N. J. Atypical p38 signaling, activation, and implications for disease. *Int. J. Mol. Sci.* **22**(8). (2021).
44. Tanno, M. et al. Diverse mechanisms of myocardial p38 mitogen-activated protein kinase activation: evidence for MKK-independent activation by a tables 1-associated mechanism contributing to injury during myocardial ischemia. *Circul. Res.* **93**(3), 254–261 (2003).
45. Fiedler, B. et al. cGMP-dependent protein kinase type I inhibits tables 1-p38 mitogen-activated protein kinase apoptosis signaling in cardiac myocytes. *J. Biol. Chem.* **281**(43), 32831–32840 (2006).
46. Jung, K. H. et al. Targeted disruption of Nemo-like kinase inhibits tumor cell growth by simultaneous suppression of Cyclin D1 and CDK2 in human hepatocellular carcinoma. *J. Cell. Biochem.* **110**(3), 687–696 (2010).
47. Yasuda, J. et al. Nemo-like kinase induces apoptosis in DLD-1 human colon cancer cells. *Biochem. Biophys. Res. Commun.* **308**(2), 227–233 (2003).
48. Zhao, J. S. et al. The novel suppresses autophagy degradation of BBC3 by preventing its interactions with HSPA8 to induce trophoblast cell apoptosis. *Autophagy* **20**(10), 2255–2274 (2024).
49. Li, Z. W. et al. The degradation of EZH2 mediated by LncRNA ANCR attenuated the invasion and metastasis of breast cancer. *Cell. Death Differ.* **24**(1), 59–71 (2017).

Acknowledgements

This work was supported in part by the Joint Project on Regional High-Incidence Diseases Research of Guangxi Natural Science Foundation (2023GXNSFAA026001); the 111 Project (D17011); the Youth Science Foundation of Guangxi Medical University (GXMUYSF202414); and the Innovation Project of Guangxi Graduate Education (YCBZ2024131).

Author contributions

Z.L. and S.H. generated the hypothesis and designed the experiments. B.P., L.L., S.C., K.H., M.L., and J.Q. performed experiments. Z.Q., J.C., L.L., and Q.X. performed the animal experiments. B.P., L.L., and Q.X. interpreted the data. Z.L., S.H., and K.H. wrote the manuscript.

Declarations

Competing interests

The authors declare no competing interests.

Ethics approval and consent to participate

All animal experiments were approved by the Committee on the Ethics of the First Affiliated Hospital of Guangxi Medical University (Approval number: 2024-E082-01) on January 27, 2023.

Additional information

Supplementary Information The online version contains supplementary material available at https://doi.org/10.1038/s41598-025-92614-4.

Correspondence and requests for materials should be addressed to S.H. or Z.L.